

Electronic Supplementary Information

Intermediate-temperature Proton Conductivity of Li⁺/H⁺ ion-exchanged material (Li,H)_{3.5}Zn_{0.25}GeO₄

Toshiaki Matsui ^{a)}, *, Takashi Ozeki ^{a)}, Kazunari Miyazaki ^{a)}, Sadahiro Nagasaka ^{a)}, Hiroki Muroyama ^{a)}, Kenichi Imagawa ^{b)}, Yoshimi Okada ^{b)}, and Koichi Eguchi ^{a)}

a) Department of Energy and Hydrocarbon Chemistry, Graduate School of Engineering, Kyoto University, Nishikyo-ku, Kyoto 615-8510, Japan. E-mail: matsui@elech.kuic.kyoto-u.ac.jp

b) Chiyoda Corporation, Nishi-ku, Yokohama 220-8765, Japan

Samples ion-exchanged in aqueous solutions

Preparation:

The Li⁺/H⁺ exchange for Pristine LZG was performed in 5, 20, 50 mM acetic acid aqueous solutions for 24 h at room temperature (powder/acetic acid = 1/40 in a weight ratio). The time course of the pH change was monitored by the pH meter (Horiba); in the case of 5 mM acetic acid, the pH reached the steady state within 5 sec from the beginning of the powder immersion in acid, indicating the rapid progress of the Li⁺/H⁺ exchange. After the immersion, the ion-exchanged powder was collected by the filtration and washed with distilled water. Then, the resultant powder was dried in air, which was denoted as Ion-exchanged LZG.

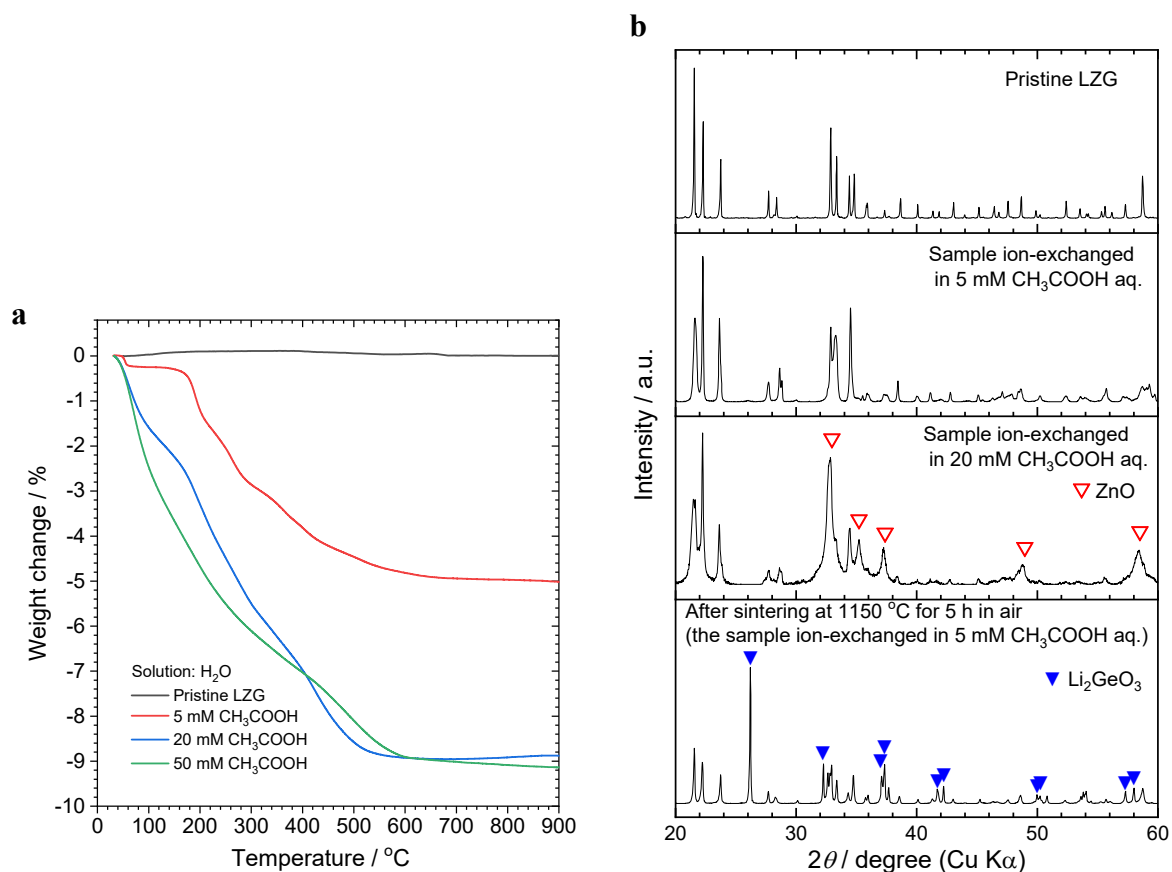


Fig. S1 Characteristics of LZG immersed in various concentrations of acetic acid aqueous solutions. (a) TGA profiles measured in air at the heating rate of 10 °C min⁻¹. (b) XRD patterns of pristine, ion-exchanged and sintered samples.

Fig. S1(a) shows TGA profiles for both Pristine and Ion-exchanged LZG powders. For Ion-exchanged LZG, a significant weight reduction was confirmed in the heating process, especially at 200-600 °C, as compared to the pristine sample. This characteristic weight loss was ascribable to the dehydration. So, the amount of exchanged H⁺ was roughly estimated for Ion-exchanged LZG, assuming that the weight loss above 100 °C was caused by the elimination of proton in the lattice. The H⁺ ratio of Ion-exchanged LZG immersed in 5 mM CH₃COOH aqueous solution was calculated to be 24.6%, which is almost comparable to that of the theoretical ratio of Li⁺ located in interstitial sites to all Li⁺ ions of Pristine LZG, 21.4%. However, the exchange ratio appears to be overestimated slightly, ca. 15%, indicating the partial decomposition of [Li₁₁Zn(GeO₄)₄]³⁻ framework. Furthermore, it can be seen that

the higher the concentration of the acetic acid aqueous solution, the more the decomposition proceeds. As shown in Fig. S1(b), the crystallinity of Ion-exchanged LZG lowered, and the impurity phase of ZnO was detected in some cases. Thus, there is a strong relationship between TGA profiles and XRD patterns. Furthermore, the sample after sintering process at 1150 °C contained the secondary phase of Li_2GeO_3 , which is reported as the low-conductive material; $\sigma_{\text{Li}^+} : 1.5 \times 10^{-5} \text{ S cm}^{-1}$ at 400 °C in O_2 .^[1] In other words, the sintered sample is the mixture of Ion-exchanged LZG and Li_2GeO_3 . Therefore, we need to develop the new strategy to fabricate the dense electrolyte without impurity phases.

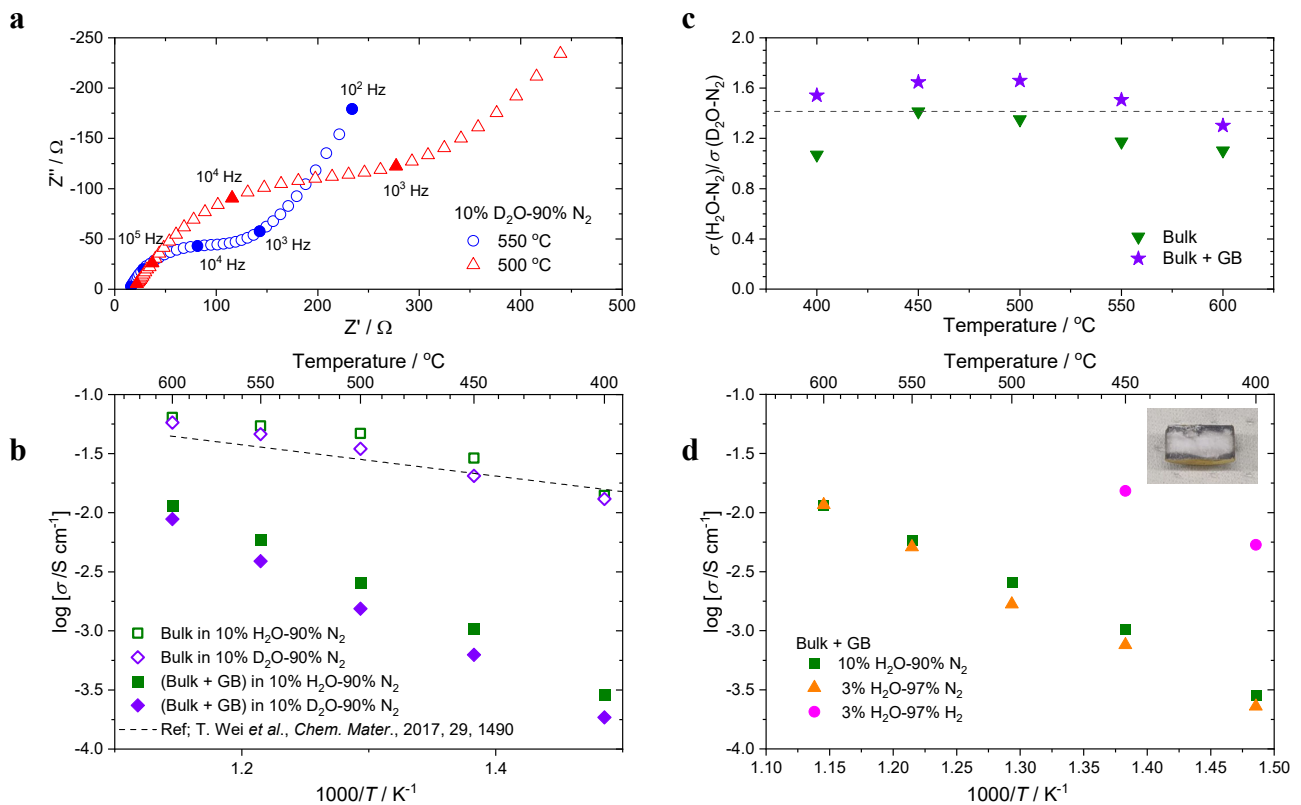


Fig. S2 Electrochemical properties of LZG ion-exchanged in a 5 mM acetic acid aqueous solution. (a) Nyquist plots measured in 10% D_2O -90% N_2 . (b) Temperature dependence of electrical conductivity in 10% H_2O -90% N_2 and 10% D_2O -90% N_2 . (c) Conductivity ratio of $\sigma(\text{H}_2\text{O}-\text{N}_2)/\sigma(\text{D}_2\text{O}-\text{N}_2)$ as a function of temperature. (d) Temperature dependence of total conductivity in various atmospheres, and the inset image of the fracture cross section of pellet after measurement in a hydrogen atmosphere. The data in (b) was referred from ref. [2].

In Nyquist plots (Fig. S2(a)), the small arc was confirmed in high frequency region at every temperature. The high-frequency intercept of real axis and the chord length of small arc were roughly assigned to the bulk resistance and grain boundary (GB) resistance, respectively. Note that the total resistance measured by dc-four probe method was almost comparable to the sum of bulk and grain boundary resistances obtained by impedance spectroscopy at 500-600 °C. The electrical conductivity ascribable to bulk was 63.9 mS cm⁻¹ and 14.0 mS cm⁻¹ at 600 °C and 400 °C, respectively, in 10% H₂O–90% N₂ as shown in Fig. S2(b). The obtained conductivity was significantly high with a low activation energy of 0.44 eV. On the other hand, the total electrical conductivity was 11.5 mS cm⁻¹ and 0.29 mS cm⁻¹ at 600 °C and 400 °C, respectively. Furthermore, the activation energy increased to 1.00 eV. These results mean that the grain boundary resistance is significantly high probably due to the formation of the secondary phase of Li₂GeO₃ as is observed in Fig. S1(b).

The H/D isotopic exchange experiment revealed that the main migration carrier in Ion-exchanged LZG is proton, as shown in Fig. S2(c). This is because the $\sigma(\text{H}_2\text{O}-\text{N}_2)/\sigma(\text{D}_2\text{O}-\text{N}_2)$ ratio was close to the theoretical ratio of $\sqrt{2}$,^[3] which originates from the difference in the mass of proton and deuteron. Fig. S2(d) shows the temperature dependence of electrical conductivity for Ion-exchanged LZG in various atmospheres. Since the conductivity ratio of $\sigma(10\% \text{ H}_2\text{O}-90\% \text{ N}_2)/\sigma(3\% \text{ H}_2\text{O}-97\% \text{ N}_2)$ was in the range of 1~1.5 depending on the temperature, this suggests a slight humidity dependency of electrical conductivity. On the other hand, a significant increase in conductivity was confirmed in 3% H₂O–97% H₂; the data above 500 °C are missing because the clear arc cannot be measured in impedance spectra. After the conductivity measurement, we found that the color of the pellet changed from white to gray and this phenomenon proceeded only at the surface of the electrolyte as shown in the inset image; *cf.*, such a color change cannot be observed after the measurement in humidified nitrogen atmospheres. As described in Fig. S1, the occurrence of excessive ion exchange may be the reason. A small amount of ZnO and/or GeO₂ would be formed upon the Li⁺/H⁺ exchange treatment, which cannot be detected by XRD analysis. These oxides will be reduced in 3% H₂O–97% H₂,

resulting in a relatively high electrical conductivity. In fact, the hydrogen consumption was observed for Ion-exchanged LZG above ca. 450 °C in the temperature programmed reduction analysis with a heating rate of 10 °C min⁻¹ in 4% H₂-96% Ar, while Pristine LZG began to be reduced at ca. 600 °C. Thus, the optimization of Li⁺/H⁺ exchange condition and/or the application of the protection layer to prevent the exposure to reducing atmospheres will be required when Ion-exchanged LZG is applied as an electrolyte of fuel cells.

Samples ion-exchanged in non-aqueous solutions

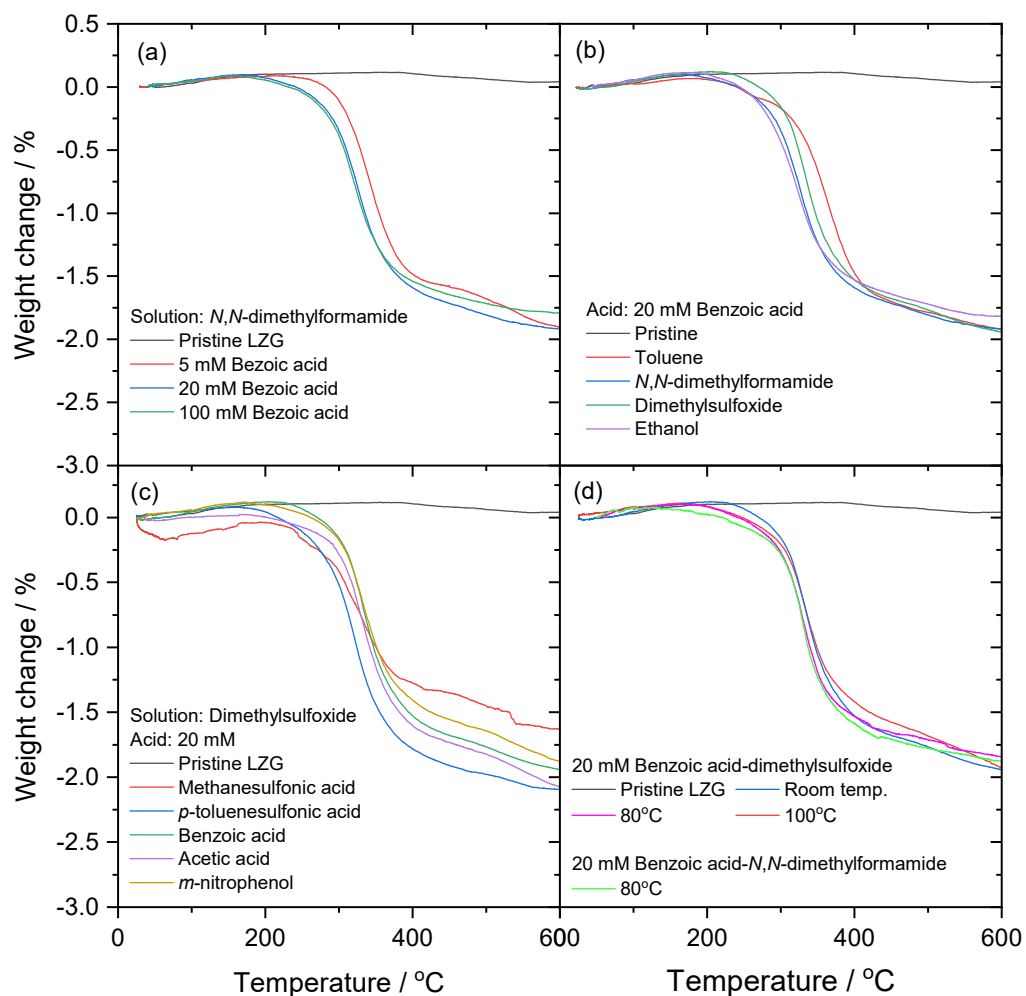


Fig. S3 TGA profiles of H-LZG ion-exchanged in various conditions by changing (a) acid concentration, (b) acid species, (c) solvents, and (d) temperature.

Table S1 Lattice parameters of Pristine LZG, and as-prepared and sintered H-LZG

	Lattice parameters		
	$a / \text{\AA}$	$b / \text{\AA}$	$c / \text{\AA}$
Pristine LZG	10.886(5)	6.276(6)	5.139(7)
H-LZG	10.877(5)	6.269(3)	5.144(2)
H-LZG sintered at 1150 °C for 5h	10.880(4)	6.276(2)	5.143(1)

Lattice parameters for H-LZG was calculated with assuming that H-LZG crystallizes in the *Pnma* orthorhombic space group, which is the same as that of Pristine LZG.^[4] By using the calculated lattice parameters and chemical formula, the density of H-LZG can be derived as 3.32 g cm⁻³. The apparent relative density of sintered H-LZG pellets was estimated to be more than 94% in this study. Thus, a series of electrical conductivity for H-LZG shown in Fig. 2 is reliable.

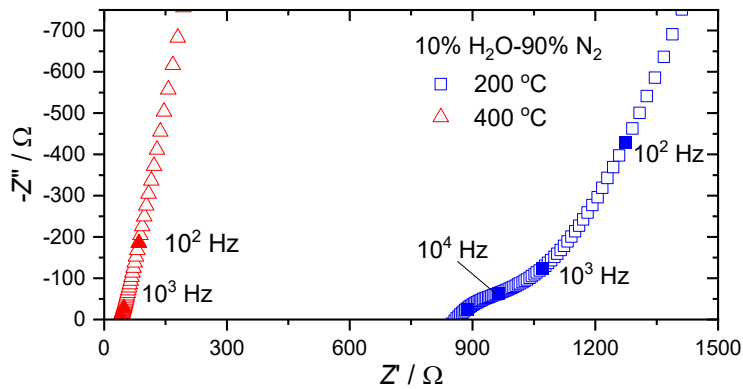


Fig. S4 Nyquist plots for H-LZG measured in 10% H₂O-90% N₂.

For H-LZG, the intercept with the real axis in the high frequency region was assigned to the bulk resistance. The semicircle related to the grain boundary resistance cannot be measured precisely above 250 °C.

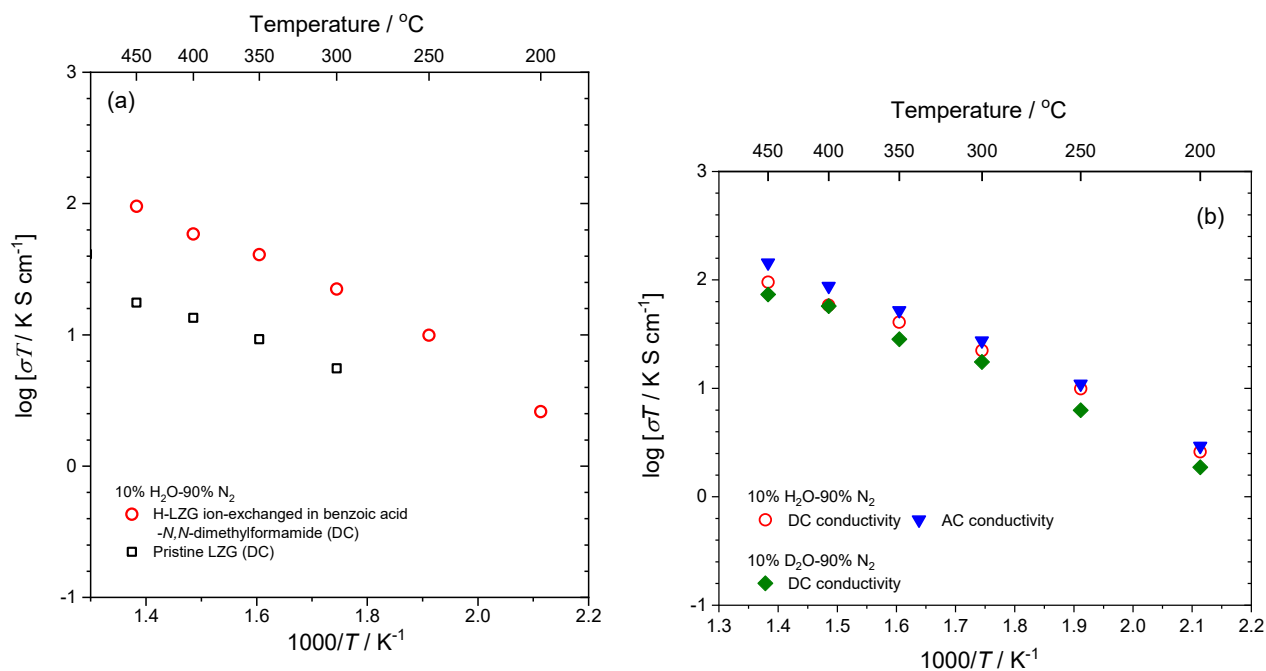


Fig. S5 (a) Arrhenius plots of electrical conductivity for H-LZG and Pristine LZG in 10% H₂O-90% N₂. (b) Arrhenius plots of electrical conductivity for H-LZG measured by AC and DC methods in 10% H₂O-90% N₂ and 10% D₂O-90% N₂.

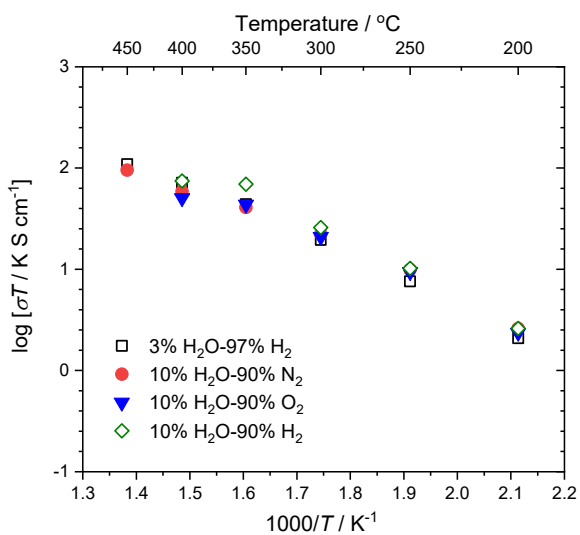


Fig. S6 Arrhenius plots of electrical conductivity for H-LZG in various atmospheres.

References

- [1] B. E. Liebert, R. A. Huggins, *Mater. Res. Bull.*, 1976, **11**, 533.
- [2] T. Wei, L. A. Zhang, Y. Chen, P. Yang, M. Liu, *Chem. Mater.*, 2017, **29**, 1490.
- [3] A. S. Nowick, A. V. Vaysleyb, *Solid State Ionics*, 1997, **97**, 17.
- [4] H. Y-P. Hong, *Mater. Res. Bull.*, 1978, **13**, 117.